LA-UR- 09-01237

Approved for public release; distribution is unlimited.

Title:	EFFECT OF DEPHASING ON DNA SEQUENCING VIA TRANSVERSE ELECTRONIC TRANSPORT
Author(s):	Matt Krems/Non-LANL Michael Zwolak/222326/T-4/LANL Yuriy Pershin/Non-LANL Massimiliano Di Ventra/Non-LANL
Intended for:	Biophysical Journal

Los Alamos
NATIONAL LABORATORY
EST. 1943

Form 836 (7/06)

Effect of Dephasing on DNA Sequencing via Transverse Electronic Transport

Matt Krems[1], Michael Zwolak[2], Yuriy V. Pershin[3], Massimiliano Di Ventra[1]

[1] *Department of Physics, University of California, San Diego, La Jolla, CA 92093*
[2] *Theoretical Division, MS-B213, Los Alamos National Laboratory, Los Alamos, NM 87545*
[3] *Department of Physics and Astronomy and USC Nanocenter, University of South Carolina, Columbia, SC 29208*

(Dated: February 25, 2009)

Previous theoretical studies have shown that, in the absence of dephasing, measuring the transverse current across DNA strands while they translocate through a nanopore or channel may provide a statistically distinguishable signature of the DNA bases, and may thus allow for rapid DNA sequencing. However, fluctuations of the environment, such as ionic and DNA motion, introduce scattering processes that give rise to dephasing. This may affect the viability of this approach to sequencing. To understand this issue, we have analyzed the role of dephasing in determining the current distributions of the DNA bases. We find that the effects of dephasing are strongly suppressed due to the off-resonant nature of tunneling through the nucleotides, and we thus expect this result to be a general feature of transport in molecular junctions. In particular, only large dephasing strengths, i.e., compared to the energetic gap between the molecular states and the Fermi level, alter the form of the current distributions and the absolute magnitude of the current. Since this gap itself is quite large, the current distributions remain protected from dephasing, further demonstrating the prospects of using transverse electronic transport measurements for DNA sequencing.

Introduction

The prospect of sequencing an entire human genome for less than $1000 US in a matter of hours is becoming closer to reality [1–3]. The original DNA-nanopore experiments of Kasianowicz et al. [4] showed that polynucleotides can be pulled through nanoscale pores and their translocation detected by measuring the consequent blockage of the ionic current through the pore. Since then, numerous experimental studies have been performed using biological [5–10] and synthetic nanopores [11–16] that probe various physical properties of translocating polynucleotides. This has fueled an enormous amount of research into novel sequencing proposals based on nanopores or nanochannels [1–3].

One sequencing idea suggests to detect transverse electron currents as single-stranded DNA (ss-DNA) translocates through a pore [17–20]. Previous theoretical work showed that the four DNA nucleotides possess distinguishable electronic signatures [17] and that these signatures produce statistically distinguishable current distributions when static structural distortions are accounted for and control on the DNA dynamics is exerted (e.g., by a transverse field of the same magnitude as that driving the current) [18–20]. These results demonstrate that DNA sequencing is in principle possible via transverse current measurements, but up until recently, no experiments had actually embedded nanoscale electrodes into a nanopore or nanochannel. Experimentalists have now successfully embedded electrodes into solid state nanopores [21] and nanochannels [22, 23] and are getting closer to measuring electronic currents with single nucleotides present in the electronic junction. When the latter is achieved, one question that will arise is how does the noise induced by the environment, i.e., noise not due only to the "static" structural distortion of the nucleotides, affect the electronic signatures, i.e., the current distributions. By "environment" we mean ionic fluctuations and other energy excitations which may drastically affect electron dynamics, and thus the current [24]. The influence of these and related factors can be very important, as seen in longitudinal electronic transport through DNA [25–27], and so far no study has examined such

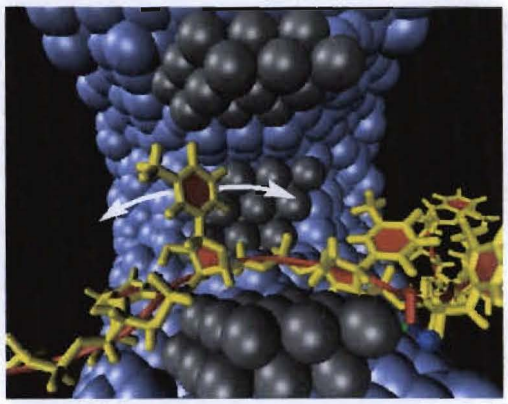

FIG. 1: Schematic representation of ss-DNA translocating through a pore while the transverse electronic current is collected. The purple atoms are the silicon nitride pore and the black atoms represent the electrode surfaces within our molecular dynamics simulations. The single strand of DNA translocates through the pore pulled by a longitudinal electric field, $E_{\parallel}$ and, while between the electrodes, the nucleotides feel a transverse electric field, $E_{\perp}$. The white arrows around the DNA base indicate an acoustic phonon-like motion that contributes to the dephasing.

effects.

In this article, we investigate the effects of one type of noise - dephasing - on the current distributions associated with the four nucleotides. Dephasing is due to noise associated with environment fluctuations at given energy scales. One might expect that this type of noise would destroy the ability of distinguishing the DNA bases once its strength is of a sufficiently large magnitude. Indeed, we do find this type of behavior. However, the noise strength at which dephasing starts to influence electronic transport is very large, beyond the strength one would expect in realistic experimental situations. This is due to the off-resonant nature of tunneling through the nucleotides, and we thus expect this result to be a general feature of molecular junctions. In other words, the separation of the energy levels of the nucleotides from the equilibrium Fermi level "protects" the electronic signature of the bases. The present study will thus help researchers understand future experimental measurements, and further demonstrates that DNA sequencing via transverse electronic transport may be a viable technology.

Setup and Methods

As our starting point, we use molecular dynamics simulations to pull homogeneous ss-DNA through a Si_3N_4 nanopore with embedded gold electrodes. Our basic setup is shown in Fig. 1. These simulations give us the real-time atomistic structure of ss-DNA as it propagates through the pore. With these structures, we calculate the electronic transport in the transverse direction across the pore. In the latter calculations, we include the effect of dephasing as discussed below.

The details of the simulations are as follows. The pore is made of 2.4 nm thick silicon nitride material in the β-phase. The nanopore hole has a double conical shape with a minimum diameter of 1.4 nm located at the center of the membrane with an outer diameter of 2.5 nm (see Fig. 1). The inner diameter is chosen wide enough such that ss-DNA is able to pass through but narrow enough that an appreciable tunneling current can be detacted. The nanopore is then solvated in a TIP3 water sphere of 6.0 nm radius with spherical boundary conditions in an NVT ensemble and with a 1 M solution of potassium and chlorine ions. The CHARMM27 force field [28, 29] is used for the interaction of DNA, water, and ions, while UFF [30] parameters are used for the interaction of the Si_3N_4 membrane and other atoms. The Si_3N_4 atoms are assumed to be fixed during the simulation (this does not affect the results). A 1 fs timestep is used and the system temperature is kept at room temperature with a Langevin dampening parameter of 0.2 ps^{-1} in the equations of motion [31]. The van der Waals interactions are cut off starting at 10 Å from each atom until reaching zero interaction at 12 Å. The energy was initially minimized in 1000 time steps.

A single strand of DNA is constructed by removing one strand from a helical, double-stranded polynucleotide created using the Nucleic Acid Builder of the AmberTools package [32]. At the initial time of the simulation, the ss-DNA is placed parallel to the pore axis with the first base just inside the pore. The ss-DNA is driven through the pore with a global electric field like that of a capacitor of 6 kcal/(mol Åe) to achieve reasonable simulation times. In the calculation of the electronic transport, the longitudinal pulling field is turned off and a transverse field (of the same magnitude as that driving the current) is turned on at a moment when a base is aligned with the electrodes. This approximates the situation when the transverse field is much larger than the longitudinal field. We envision this as the typical operating regime for a sequencing device as it allows for the suppression of a significant amount of structural distortion [18]. The particular time to stop the translocation is chosen by visual inspection, after which an energy minimization is again performed for 1000 time steps. The particular stopping time is not important because it only takes on the order of 100 ps for the transverse field, $E_\perp$, to align the nucleotide with the electrodes [19]. Single-stranded DNA differs from double-stranded DNA in that the persistence length of the polynucleotide is much shorter. This, in particular, allows for the base to quickly align with the perpendicular electric field.

The current calculations are performed within a single-particle scattering approach using a tight-binding Hamiltonian (see, e.g., Ref. [24]). These calculations include water although it was shown previously that the water has only a small direct effect on the current [19]. "Snapshots" of the atomistic structure of ss-DNA between the gold electrodes are taken from the molecular dynamics at regular time intervals. These coordinate snapshots are used to obtain the tight-binding Hamiltonian. For each carbon, nitrogen, oxygen, and phosphorous atom, s, p_x, p_y, p_z orbitals are used, whereas for gold and hydrogen only s orbitals are employed. The Fermi level is taken to be that of bulk gold [37].

To obtain the current across the ss-DNA, we use the retarded Green's function

$$G_{DNA}(E) = \frac{1}{ES_{DNA} - H_{DNA} - \Sigma_t - \Sigma_b - \Sigma_{dp}}, \quad (1)$$

where E is the energy, S_{DNA} and H_{DNA} are the overlap and Hamiltonian matrices, respectively, of the contents of the electronic junction, $\Sigma_{t(b)}$ are the self-energy terms associated with the interaction between the electrodes and the junction contents, and Σ_{dp} is the self-energy associated with dephasing. The Green's function for gold needed to calculate $\Sigma_{t(b)}$ is approximated as in Ref. [33]. We use a white-noise dephasing term, which corresponds

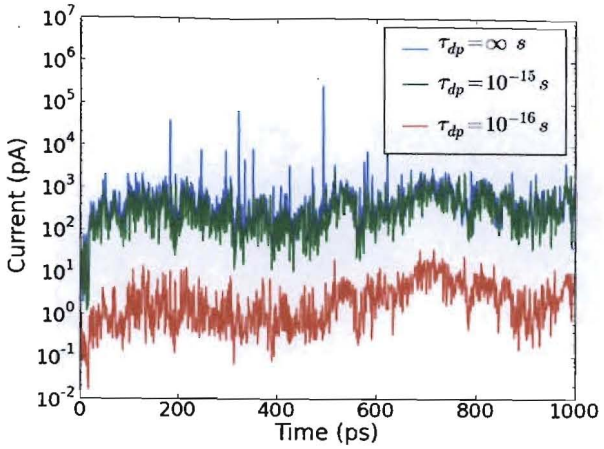

FIG. 2: Transverse current versus time for poly(A)$_{15}$ at a transverse bias voltage of 1.0 V. The dephasing lowers the current slightly for $\tau_{dp} = 10^{-15}$ s. Only at the unrealistic $\tau_{dp} = 10^{-16}$ s does the current shift significantly. Slower dephasing timescales give essentially the same current as the case with an infinite dephasing timescale.

to a dephasing timescale via

$$\tau_{dp} = -\frac{\hbar}{\mathrm{Im}\{\Sigma_{dp}\}}, \tag{2}$$

and we also take $\mathrm{Re}\{\Sigma_{dp}\} = 0$ (dephasing due to low-energy excitations, see also discussion below). For a given G_{DNA}, the transmission coefficient is

$$T(E) = Tr\left[\Gamma_t G_{DNA} \Gamma_b G_{DNA}^{\dagger}\right], \tag{3}$$

where $\Gamma_{t(b)} = i\left(\Sigma_{t(b)} - \Sigma_{t(b)}^{\dagger}\right)$. The current is then given by

$$I = \frac{2e}{h}\int_{-\infty}^{\infty} dE T(E)\left[f_t(E) - f_b(E)\right], \tag{4}$$

where $f_{t(b)}$ is the Fermi-Dirac function of the top (bottom) electrode [24]. The current distributions for the nucleotide is the distribution obtained from the various snapshots while the nucleotide fluctuates between the electrodes.

Dephasing - As stated above, previous theoretical studies have shown that the current distributions caused by DNA static structural distortions are statistically distinguishable [17–20]. These studies, however, have not included the effects of external noise, such as dephasing. We focus specifically on dephasing given by Eq. 2 because it represents fluctuations of the environment at all energy scales, which incorporates many processes that happen in experiment. These include fast processes, such as electronic interactions with bound waters or charges on the pore walls, and also slow processes, such as the dynamic movement of the DNA bases. From visual inspection of the molecular dynamics simulations, we observe that the bases fluctuate in a way reminiscent of acoustic phonons, i.e., we observe only low-energy excitations. An example of these excitations is represented in Fig. 1, where these slow oscillations, while not periodic, are mostly in the longitudinal direction. No oscillations where the bases are, e.g., in a "breathing mode", that is where the base itself is expanding and contracting, causing large energy relaxation, were observed. These are also unlikely to be excited at low bias so that we expect a low exchange of energy with the current-carrying electrons [34, 35]. Therefore, the dominant effect of these slow processes, as with the fast processes, must be a change in the phase of the electron wavefunctions and not dissipation/heating. Furthermore, we assume the dephasing term, Eq. 2, is a constant for all molecular states in the junction. In certain cases, this most likely overestimates the strength of the noise, but, on the other hand, misses "colored noise" effects, where, for instance, the noise has a strong component at a particular frequency. In the absence of a physical model for such noise which is supported by experiments, its effect is only speculative and we thus defer its study for future research.

Results and Discussions

We have performed current calculations for some representative dephasing timescales [36]: $\tau_{dp} = \infty, 10^{-13}, 10^{-14}, 10^{-15}, 10^{-16}$ s with transverse voltages of 0.1 V and 1.0 V. The dephasing timescale of 10^{-16} s is a particularly fast and unphysical timescale but was used to show the onset of major differences in the current and current distributions.

For slow dephasing, ($\tau_{dp} = 10^{-13}$s - 10^{-14}s), the average current itself is essentially unchanged as well as the distributions. The average percent change of an individual current value for $\tau_{dp} = 10^{-13}$ s is only about 0.1 %. For $\tau_{dp} = 10^{-14}$ s, it is 1.5 %. However, for a single current value, the current may vary by orders of magnitude due to dephasing, further strengthening the argument that a single base measurement is likely not enough to distinguish the bases [18]. From Figs. 2 and 3, a $\tau_{dp} = 10^{-15}$ s lowers the current on average and slightly alters the distributions. There is an average current reduction of about 30 %. At the unphysical fast timescale of 10^{-16}s, the current is significantly lowered and the distributions are pushed into an unmeasurable regime. However, we are not aware of a physical process that may cause such a fast dephasing under the experimental conditions envisioned in this work.

We present results for the cases of 0.1 V and 1.0 V transverse biases. Previous work has shown that the transverse bias has a nonlinear effect on the mean of the distribution [19]. This is due to both a pulling ef-

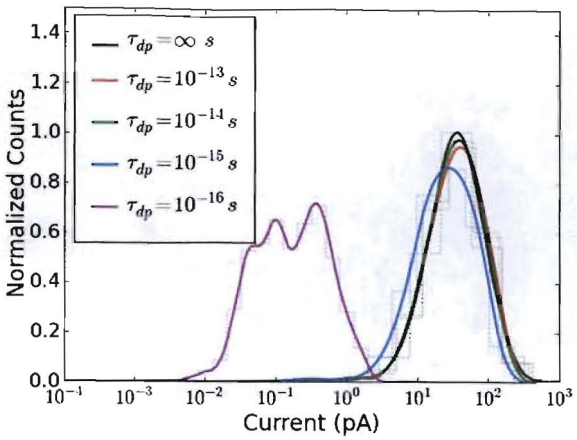

FIG. 3: Probability distributions for poly(A)$_{15}$ with various dephasing timescales for a transverse bias voltage of 1.0 V. The very light dashed lines correspond to the bins used to produce the current distributions. The solid lines are interpolated from the dashed ones. Like the current itself, only at the unrealistic $\tau = 10^{-16}$ s does the distribution change and shift appreciably. At $\tau = 10^{-15}$ s, the distribution's mean shifts slightly, and it broadens somewhat.

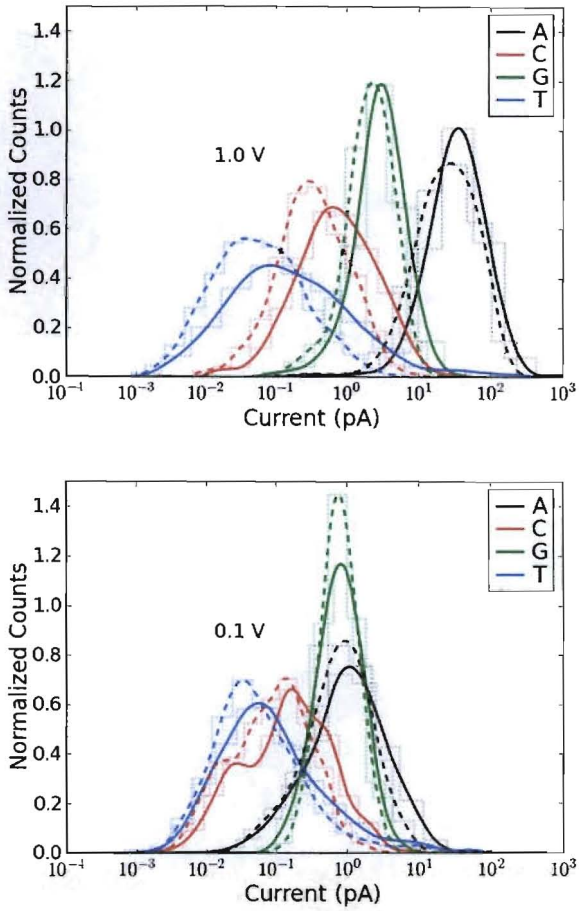

FIG. 4: Normalized current distributions for the four nucleotides at a transverse bias voltage of 1.0 V (top) and 0.1 V (bottom). The solid lines correspond to an infinite dephasing timescale (no dephasing) and the dark dashed lines represent the distributions for $\tau_{dp} = 10^{-15}$ s, with the light dashed lines representing the bins uses to produce the distributions. One can see that all of the distributions are shifted somewhat to lower current values corresponding to an overall lowering of the current magnitude. However, the distributions themselves are very similar to the case of an infinite dephasing timescale.

fect of the backbone toward one electrode as the field is increased with consequent alignment of the base toward the other electrode, and the steric effect of the alignment of the backbone with one of the electrodes. Therefore, while one can expect the mean current to be shifted to lower values with lower bias, the degree to which this occurs is not easy to determine *a priori*. This is especially true with the smaller bases like T. For this base, one cannot always expect perfect alignment at all times with the electrodes even in the presence of a stabilizing transverse field, further emphasizing the statistical nature of this problem.

Model - As found above, even a relatively strong dephasing does not alter the average current, or current distributions, too much. This may seem an unexpected result and it will be helpful for future experimental and theoretical efforts to understand the reason for such an effect. For the remainder of this paper, we thus develop a model system to understand this behavior, which shows good agreement with the above computational results. Our starting point is based on our previous work on transverse transport through DNA [17–20]. In an ideal configuration of a nucleotide between electrodes, the LUMO level of the base is closest to the gold Fermi level [1, 17] and also couples well to both electrodes. Thus, it is reasonable to treat a nucleotide in the electronic junction as a single energy level, E_0. In order to get an analytical model, we make further approximations. First, we assume that the system is at low temperature and we work in the linear response regime so that the electrodes can be treated as having an infinite bandwidth. Second, we assume the junction energy level is equally coupled to all levels of both electrodes. Within these approximations, the retarded Green's function, Eq. 1, becomes

$$G_{DNA}(E) = \frac{1}{E - E_0 + i\gamma + i\eta}, \tag{5}$$

where γ represents twice the coupling strength to a single electrode, and $\eta = \hbar/\tau_{dp}$. For $\gamma \ll E_0$, this expression, using Eq. 3 and Eq. 4, gives

$$I(\eta) \approx \frac{2e^2V}{h} \frac{\gamma^2}{E_0^2 + \eta^2} \tag{6}$$

i.e., the current for just a single structural distortion in linear response and weak coupling.

We know from above, that the current acquires a distribution when structural distortions of the DNA are taken into account. Under the assumptions that went into Eq. 5 we can introduce these structural distortions by allowing E_0 or γ to acquire distributions. From Fig. 3, it is clear that the current distributions on a logarithmic scale could be approximated as a Gaussian when no dephasing is present, which indicates that the coupling to the electrodes is controlling these distributions, as only the coupling fluctuates on an exponential scale. By assuming the coupling to both electrodes identical, we miss structural distortions that bring the base into closer proximity to one electrode and farther from the other. However, this is unlikely to affect the essential physics.

Now, let us calculate the distribution of γ's using the curve in Fig. 3 with no dephasing. Using the fact that the current distribution in a logarithmic scale is Gaussian, and that we are in a weak coupling regime ($\gamma \ll E_0$), $\ln \gamma/\gamma_m$, where γ_m is the maximum, should also be Gaussian distributed,

$$p(\ln \gamma/\gamma_m) = \frac{1}{\sigma_{\gamma/\gamma_m}\sqrt{2\pi}} \exp\left\{-\frac{(\ln \gamma/\gamma_m)^2}{2\sigma^2_{\gamma/\gamma_m}}\right\}, \quad (7)$$

with the standard deviation $\sigma_{\gamma/\gamma_m} = \sigma_{I(0)}/2 \approx 0.5$, where $\sigma_{I(0)}$ is the standard deviation of the current with $\eta = 0$. The maximum, $\ln \gamma_m$, appears at -7.2, when $E_0 = 1\,\text{eV}$, which is approximately the energy separation of Adenine's LUMO from gold's Fermi level [1]. We assume that the standard deviation of $\ln \gamma/\gamma_m$ does not change when we turn on dephasing. Thus, the only thing that can happen is that the logarithmic distribution of $I(\eta)$ shifts to lower currents with increasing η. This is plotted in Fig. 5.

Although we assume in our model that the distribution stays Gaussian with the same standard deviation no matter what the dephasing strength, our model explains the key features found in our numerical simulations. Small dephasing does not affect the current because we are in an off-resonant tunneling regime. The fact that the current is relatively insensitive to the dephasing even for fairly strong dephasing is because the molecular energy levels are far away from the gold Fermi level. This is represented by the Lorentzian $(E_0^2 + \eta^2)^{-1}$ in the current. The other features that develop, increased broadening and eventual multiple peak development, are not explained by our simple model. These are due to multiple energy levels, i, contributing to transport. The contribution from each reaches its turning point, $\eta \approx E_i$ at a different value of η and thus the single peak broadens and develops into multiple peaks.

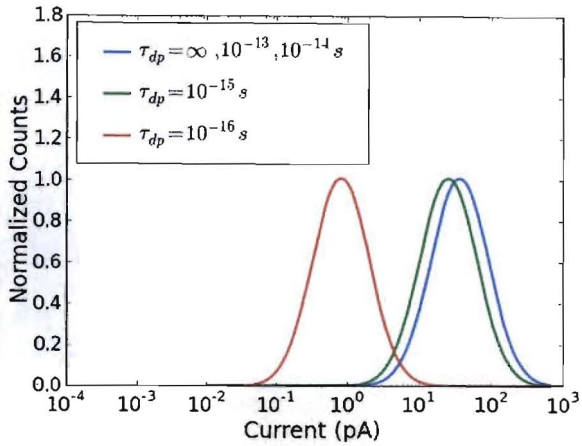

FIG. 5: Current distributions of a model system for the Adenine nucleotide represented by a single energy level E_0. The current distribution on a logarithmic scale is taken to be Gaussian as in Fig. 3 for no dephasing. As dephasing is turned on, at first the distribution does not change at all, but around $\eta \approx E_0$, where $\eta = \hbar/\tau_{dp}$ measures the strength of the dephasing, the distribution starts to shift. At larger η, the peak of distribution shifts to lower values as η^{-2}. The off-resonant tunneling, indicated by large E_0 as measured from the Fermi level, "protects" the current distributions from dephasing.

Conclusion

In conclusion, we have presented results combining molecular dynamics simulations with quantum mechanical current calculations including dephasing. We have shown that for reasonable dephasing timescales, e.g., down to $10^{-15}\,\text{s}$, dephasing will likely not affect the distinguishability of the current distributions obtained from measuring the transverse electronic current of the different DNA nucleotides. At extremely fast dephasing timescales, below $10^{-15}\,\text{s}$, the distributions are significantly altered, but this is beyond physically reasonable dephasing times for the experimental system we are considering. We have also proposed a simple model system that provides insight into the reason the electronic signatures are relatively insensitive to dephasing. This is due to the off-resonant nature of tunneling through the nucleotides and thus it is likely to be a general property of transport in organic molecules. While the distributions are only mildly affected, we have shown that dephasing can potentially alter a single current value significantly, further supporting the notion that only a statistical study of the transverse currents can potentially distinguish the nucleotides. We finally note that while our study is done for a nanopore geometry, the results are applicable to other types of sequencing devices as well, such as the nanochannels of Ref. [23] used in transverse electronic measurements.

We thank Yonatan Dubi and Johan Lagerqvist for use-

ful suggestions. This research is supported by the NIH-National Human Genome Research Institute and by the U.S. Department of Energy through the LANL/LDRD Program.

---

[1] Zwolak, M., and M. Di Ventra. 2008. Physical approaches to dna sequencing and detection. *Rev. Mod. Phys.* 80:141–165.

[2] Schloss, J. A. 2008. How to get genomes at one ten-thousandth the cost. *Nat. Biotechnol.* 26:1113–1115.

[3] Branton, D., D. W. Deamer, A. Marziali, H. Bayley, S. A. Benner, T. Butler, M. Di Ventra, S. Garaj, A. Hibbs, X. Huang, S. B. Jovanovich, P. S. Krstic, S. Lindsay, X. S. Ling, C. H. Mastrangelo, A. Meller, J. S. Oliver, Y. V. Pershin, J. M. Ramsey, R. Riehn, G. V. Soni, V. Tabard-Cossa, M. Wanunu, M. Wiggin, and J. A. Schloss. 2008. The potential and challenges of nanopore sequencing. *Nat. Biotechnol.* 26:1146–1153.

[4] Kasianowicz, J. J., E. Brandin, D. Branton, and D. W. Deamer. 1996. Characterization of individual polynucleotide molecules using a membrane channel. *Proc. Natl. Acad. Sci. U.S.A.* 93:13770–13773.

[5] Akeson, M., D. Branton, J. Kasianowicz, E. Brandin, and D. Deamer. 1999. Microsecond time-scale discrimination among polycytidylic acid, polyadenylic acid, and polyuridylic acid as homopolymers or as segments within single rna molecules. *Biophys. J.* 77:3227–3233.

[6] Meller, A., L. Nivon, E. Brandin, J. Golovchenko, and D. Branton. 2000. Rapid nanopore discrimination between single polynucleotide molecules. *Proc. Natl. Acad. Sci. U.S.A.* 97:1079–1084.

[7] Meller, A., L. Nivon, , and D. Branton. 2001. Voltage-driven dna translocations through a nanopore. *Phys. Rev. Lett.* 86:3435.

[8] Mathe, J., A. Aksimentiev, D. Nelson, K. Schulten, and A. Meller. 2005. Orientation discrimination of single-stranded dna inside the alpha-hemolysin membrane channel. *Proc. Natl. Acad. Sci. U.S.A.* 102:12377–12382.

[9] Butler, T., J. Gundlach, and M. Troll. 2006. Determination of rna orientation during translocation through a biological nanopore. *Biophys. J.* 90:190–199.

[10] Astier, Y., O. Braha, and H. Bayley. 2006. Toward single molecule dna sequencing: Direct identification of ribonucleoside and deoxyribonucleoside 5'-monophosphates by using an engineered protein nanopore equipped with a molecular adapter. *J. Am. Chem. Soc.* 128:1705–1710.

[11] Li, J., M. Gershow, D. Stein, E. Brandin, and J. Golovchenko. 2003. Dna molecules and configurations in a solid-state nanopore microscope. *Nat. Mater.* 2:611–615.

[12] Chen, P., J. Gu, E. Brandin, Y. Kim, Q. Wang, and D. Branton. 2004. Probing single dna molecule transport using fabricated nanopores. *Nano Lett.* 4:2293–2298.

[13] Storm, A., C. Storm, J. Chen, H. Zandbergen, , J.-F. Joanny, and C. Dekker. 2005. Fast dna translocation through a solid-state nanopore. *Nano Lett.* 5:1193–1197.

[14] Fologea, D., M. Gershow, B. Ledden, D. McNabb, J. Golovchenko, and J. Li. 2005. Detecting single stranded dna with a solid state nanopore. *Nano Lett.* 5:1905–1909.

[15] Chang, H., F. Kosari, G. Andreadakis, M. Alam, G. Vasmatzis, and R. Bashir. 2004. Dna-mediated fluctuations in ionic current through silicon oxide nanopore channels. *Nano Lett.* 4:1551–1556.

[16] Heng, J., C. Ho, T. Kim, R. Timp, A. Aksimentiev, Y. Grinkova, S. Sligar, K. Schulten, and G. Timp. 2004. Sizing dna using a nanometer-diameter pore. *Biophys. J.* 87:2905–2911.

[17] Zwolak, M., and M. Di Ventra. 2005. Electronic signature of dna nucleotides via transverse transport. *Nano Lett.* 5:421–424.

[18] Lagerqvist, J., M. Zwolak, and M. Di Ventra. 2006. Fast dna sequencing via transverse electronic transport. *Nano Lett.* 6:779–782.

[19] Lagerqvist, J., M. Zwolak, and M. Di Ventra. 2007. Influence of the environment and probes on rapid dna sequencing via transverse electronic transport. *Biophys. J.* 93:2384–2390.

[20] Lagerqvist, J., M. Zwolak, and M. Di Ventra. 2007. Comment on characterization of the tunneling conductance across dna bases. *Phys. Rev. E.* 76:013901–1 – 013901–3.

[21] Gierhart, B. C., D. G. Howitt, S. J. Chen, Z. Zhu, D. E. Kotecki, R. L. Smith, and S. D. Collins. 2008. Nanopore with transverse nanoelectrodes for electrical characterization and sequencing of dna. *Sens. Actuators, B.* 132:593–600.

[22] Fischbein, M. D., and M. Drndiċ. 2007. Sub-10 nm device fabrication in a transmission electron microscope. *Nano Lett.* 7:1329–1337.

[23] Liang, X., and S. Y. Chou. 2008. Nanogap detector inside nanofluidic channel for fast real-time label-free dna analysis. *Nano Lett.* 8:1472–1476.

[24] Di Ventra, M. 2008. Electrical Transport in Nanoscale Systems. Cambridge University Press.

[25] Zwolak, M., and M. Di Ventra. 2004. *In* Encyclopedia of Nanoscience and Nanotechnology. H. S. Nalwa, editor, volume X. American Scientific Publishers. 1–19.

[26] Endres, R., D. Cox, and R. Singh. 2004. The quest for high-conductance dna. *Rev. Mod. Phys.* 76:195–214.

[27] Shapir, E., H. Cohen, A. Calzolari, C. Cavazzoni, D. A. Ryndyk, G. Cuniberti, A. Kotylyar, R. Di Felice, and D. Porath. 2008. Electronic structure of single dna molecules resolved by transverse scanning tunnelling spectroscopy. *Nat. Mater.* 7:68–74.

[28] Foloppe, N., and J. Alexander D. Mackerell. 2000. All-atom empirical force field for nucleic acids: I. parameter optimization based on small molecule and condensed phase macromolecular target data. *J. Comp. Chem.* 21:86–104.

[29] Alexander D. Mackerell, J., and N. K. Banavali. 2000. All-atom empirical force field for nucleic acids: Ii. application to molecular dynamics simulations of dna and rna in solution. *J. Comp. Chem.* 21:105–120.

[30] Wendel, J. A., and W. A. G. III. 1992. The hessian biased force field for silicon nitride ceramics: Predictions of thermodynamic and mechanical properties for alpha- and beta-si3n4. *J. Chem. Phys.* 97:5048–5062.

[31] Aksimentiev, A., J. B. Heng, G. Timp, and K. Schulten. 2004. Microscopic kinetics of dna translocation through synthetic nanopores. *Biophys. J.* 87:2086–2097.

[32] Macke, T., and D. Case. 1997. *In* Molecular Modeling of Nucleic Acids. N. B. Leontis, and J. SantaLucia, editors. American Chemical Society.

[33] Pecchia, A., M. Gheorghe, A. Di Carlo, P. Lugli, T. Niehaus, T. Frauenheim, and R. Scholz. 2003. Role of thermal vibrations in molecular wire conduction. *Phys.*

Rev. B. 68:235321–1 – 235321–12.

[34] Chen, Y., M. Zwolak, and M. Di Ventra. 2003. Local heating in nanoscale conductors. *Nano Lett.* 3:1691–1694.

[35] Chen, Y., M. Zwolak, and M. Di Ventra. 2004. Inelastic currentvoltage characteristics of atomic and molecular junctions. *Nano Lett.* 4:1709–1712.

[36] Zwolak, M., and M. D. Ventra. 2002. Dna spintronics. *Appl. Phys. Lett.* 81:925–927.

[37] The tight-binding Hamiltonian is constructed at every snapshot using the YAEHMOP package (http://yaehmop.sourceforge.net/), with the Fermi level also consistently calculated using this method.